

# Enhanced summer convection explains observed trends in extreme subdaily precipitation in the northeastern Italian Alps

Eleonora Dallan<sup>1,1</sup>, Marco Borga<sup>2,2</sup>, Mattia Zaramella<sup>3,3</sup>, and Francesco Marra<sup>4,4</sup>

<sup>1</sup>University of Padua

<sup>2</sup>Università di Padova, University of Padova

<sup>3</sup>University of Padova

<sup>4</sup>Institute of Atmospheric Sciences and Climate, National Research Council

December 1, 2022

## Abstract

Understanding past changes in precipitation extremes could help us predict their dynamics under future conditions. We present a novel approach for analyzing trends in extremes and attributing them to changes in the local precipitation regime. The approach relies on the separation between intensity distribution and occurrence frequency of storms. We examine the relevant case of the eastern Italian Alps, where significant trends in annual maximum precipitation over the past decades were observed. The model is able to reproduce observed trends at all durations between 15 minutes and 24 hours, and allows to quantify trends in extreme return levels. Despite the significant increase in storms occurrence and typical intensity, the observed trends can be only explained considering changes in the tail heaviness of the intensity distribution, that is the proportion between heavy and mild events. Our results suggest these are caused by an increased proportion of summer convective storms.

Enhanced summer convection explains observed trends in extreme subdaily precipitation in the northeastern Italian Alps

E. Dallan<sup>1</sup>, M. Borga<sup>1</sup>, M. Zaramella<sup>1</sup>, F. Marra<sup>2</sup>

<sup>1</sup>Department of Land Environment Agriculture and Forestry, University of Padova, Padova, Italy

<sup>2</sup> National Research Council of Italy - Institute of Atmospheric Sciences and Climate (CNR-ISAC), Bologna, Italy

Corresponding author: Eleonora Dallan (*eleonora.dallan@unipd.it*)

## Key Points:

- We present a method for analyzing extreme precipitation trends based on the separation of storm intensity and occurrence frequency
- Our approach reproduces observed trends in annual maxima and allows to quantify trends on rare return levels
- Observed trends in the eastern Italian Alps are explained by an increased proportion of heavy convective storms in the summer

## Abstract

Understanding past changes in precipitation extremes could help us predict their dynamics under future conditions. We present a novel approach for analyzing trends in extremes and attributing them to changes in the local precipitation regime. The approach relies on the separation between intensity distribution and

occurrence frequency of storms. We examine the relevant case of the eastern Italian Alps, where significant trends in annual maximum precipitation over the past decades were observed. The model is able to reproduce observed trends at all durations between 15 minutes and 24 hours, and allows to quantify trends in extreme return levels. Despite the significant increase in storms occurrence and typical intensity, the observed trends can be only explained considering changes in the tail heaviness of the intensity distribution, that is the proportion between heavy and mild events. Our results suggest these are caused by an increased proportion of summer convective storms.

## Plain Language Summary

Quantifying past trends in extreme rainfall is important because it can help us understand future changes caused by global warming. Climate scientists and hydrologists use specific statistical models to do so, but interpreting the results is complicated because extremes are rare and the structure of the models is not linked to the local meteorology. We use a new statistical model that allows to better understand the mechanisms behind the trends we detect. We find that extreme rainfall in the eastern Italian Alps increased over the past decades and we associate this change to an increased proportion of summer thunderstorms.

## 1 Introduction

Understanding past and future changes in extreme subdaily precipitation intensities is of enormous interest because they are responsible for flash floods, urban floods, landslides and debris flows, and cause numerous casualties and huge damages every year (Borga et al., 2014; Cristiano et al., 2017; Paprotny et al., 2018). Physical laws translate increasing atmospheric temperature into increasing water vapor holding capacity. Together with changes in the atmospheric dynamics, this is expected to drive future precipitation changes (Trenberth et al., 2003; Pendergrass et al., 2020; Fowler et al., 2021b). In general, larger responses are expected for precipitation extremes because mean precipitation, on a global scale, is limited by energy constraints (Allan and Soden, 2008; Pendergrass & Hartmann, 2014). However, detecting changes in extreme precipitation is highly affected by the stochastic uncertainty characterizing the sampling of extremes. This uncertainty may mask the influence of climate forcing on the processes which locally control the extremes (Fatichi et al., 2016; Marra et al., 2019).

Statistically significant changes in the frequency of extreme precipitation in the past decades were reported, often with stronger trends in subdaily extremes, as opposed to daily (Guerreiro et al., 2018; Markonis et al., 2019; Papalexiou & Montanari, 2019). In some cases, opposing trends between short and long durations emerged, with complex implications for flood risk (Zheng et al., 2015). Available observations show different temporal trends for precipitation intensities associated to different exceedance probabilities (Schär et al., 2016; Pendergrass, 2018). In general, increasing trends are reported for rarer events (Myhre et al., 2019), but the specific differences depend on duration, season, and local conditions, such as the dominating meteorological features contributing extremes (Blanchet et al., 2021; Moustakis et al., 2021). Extreme return levels characterized by different exceedance probabilities are thus changing at different rates (Myhre et al., 2019; Marra et al., 2021).

Nonstationary extreme value models could aid the detection and quantification of trends in extreme precipitation of different exceedance probability (e.g., Min et al. 2009). However, the information these models can provide is impacted by stochastic uncertainties (Serinaldi and Kilsby, 2015; Fatichi et al., 2016), and their flexibility is limited by the assumptions concerning high order statistical moments. In fact, due to intrinsic limitations in parameter estimation accuracy, the shape (and sometimes also the scale) parameter of the extreme value distribution is usually assumed to be constant (Prosdocimi and Kjeldsen, 2021). Additionally, due to the structure of these statistical models, a link between the properties of the underlying process, such as precipitation occurrence frequency and intensity distribution, and extremes is difficult to establish (e.g. Marra et al., 2019). As such, the possibility to attribute the observed changes to specific physical and meteorological processes is hampered.

This background suggests that there is a need to move beyond traditional trend detection techniques applied to extremes only and develop novel methodologies. These methods should be able to detect general changes

in extreme precipitation at multiple durations, quantify changes at different exceedance probabilities, and attribute these to changes in the underlying physical processes.

Miniussi and Marani (2020) proposed the so-called Metastatistical Extreme Value approach (Marani and Ignaccolo, 2015) as a viable way for addressing these issues. The idea relies on the concept of *ordinary events*, that is all the independent realizations of a process of interest, and proved highly effective in reducing stochastic uncertainties (Zorzetto et al., 2016; Marra et al., 2018). As opposed to traditional methods, the distribution describing the ordinary events is assumed to be known, and the extreme value distribution is derived by explicitly considering the occurrence frequency of the ordinary events. Miniussi and Marani (2020) provided an example application in which extreme return levels were computed over moving time windows, highlighting temporal changes that could not be appreciated using traditional methods. The adopted ordinary events (daily precipitation amounts), however, were not directly connected with meteorological systems, so that direct relations between changes in extremes and changes in the underlying storm properties is still missing.

Here, we combine a novel approach for ordinary-events-based precipitation frequency analyses across durations (Marra et al., 2020) with a regional trend detection technique to: (a) detect and quantify trends in sub-daily annual maxima and extreme return levels by independently considering the changes in properties and occurrence frequency of storms, and (b) attribute the observed trends in extremes to specific changes in the local precipitation regime. We examine the relevant case of the eastern Italian Alps, where consistent significant changes in annual maximum precipitation intensities at subdaily and daily duration were reported (Libertino et al., 2019).

## 2 Data and methodology

### 2.1 Study area and data

We focus on Trentino, a 6000 km<sup>2</sup>-wide mountainous area in the Eastern Italian Alps (**Figure 1 a**) which experienced significant increases in extreme short-duration rain intensities over the last decades (Libertino et al., 2019). Mean annual precipitation varies from ~1300 mm yr<sup>-1</sup> in the south-eastern portion of the area to lower amounts (~900 mm yr<sup>-1</sup>) typical of the “inner alpine province” in the north (Borga et al., 2005). A dense network of more than one hundred rain gauges is present. From these, 30 stations (density ~1/200 km<sup>2</sup>) with at least 27 complete years (<10% missing data) of 5-minute resolution data in the period 1991-2020 are selected (**Figure 1 a**; see Table S1 in the Supporting Information).

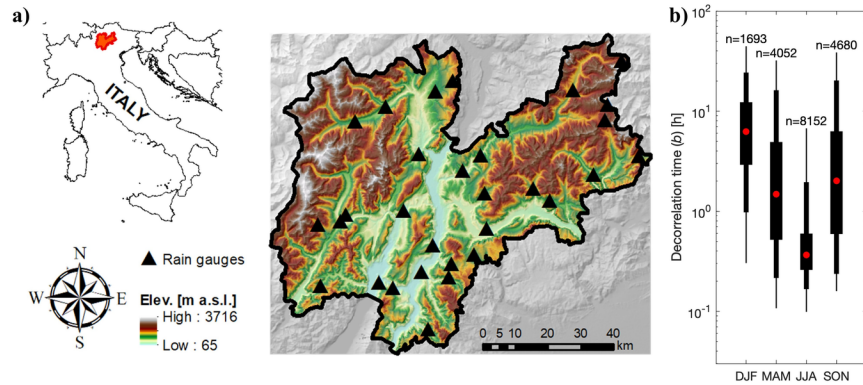


**Figure 1 . a)** Location and orography of the study area and location of the rain gauges used in this study; **b)** Decorrelation time of the highest 25% ordinary events organized by season. The red dots indicate the median values; bars indicates percentiles: 25-75th, 5-95th, 1-99th. The number of storms occurred across the stations in each season is reported.

## 2.2 Definition of the ordinary events

Ordinary events are all the independent realizations of a process of interest, in our case precipitation intensities at multiple durations. The here presented analysis is based on the storm-based identification of ordinary events proposed by Marra et al. (2020), in which “storms” are defined as independent meteorological objects, and “ordinary events” of each duration are extracted from the storms. For each station, storms are defined as wet periods separated by dry hiatuses of predefined length. We define as wet all the 5 min time intervals reporting at least 0.1 mm of precipitation, and separate storms using 24 hr dry hiatuses. A minimum duration of 30 min for a single storm is set to avoid individual tips to be considered as storms. Ordinary events are then defined as the maximum intensities observed over the duration of interest in each storm (details in Marra et al., 2020). Durations between 15 min to 24 hr are explored: 15 min, 30 min, 45 min, 1 h, 2 h, 3 h, 6 h, 12 h, 24h.

## 2.3 Tail of the ordinary events distribution

Previous studies show that subdaily precipitation intensities require three- (or more) parameters distributions (Papalexiou et al., 2018). However, their right tails can be well approximated using a two-parameter distribution which, in many cases, is found to be a Weibull distribution (e.g., Zorretto et al. 2016; Marra et al., 2020). This means that a portion of their distribution including the extremes, which is here termed “tail”, can be approximated as  $F(x; \lambda, \kappa) = 1 - e^{-\left(\frac{x}{\lambda}\right)^\kappa}$ , where  $\lambda$  is a scale parameter and  $\kappa$  is a shape parameter which determines the tail heaviness. Larger shape parameters are associated to lighter tails, and vice versa (see Figure S1). In particular, the tail is sub-exponential for  $\kappa > 1$ , exponential for  $\kappa=1$ , and heavier than exponential for  $\kappa < 1$ .

The choice of the left-censoring threshold follows the test described in Marra et al. (2020): the distribution parameters are estimated for different thresholds by censoring the values below the left-censoring threshold as well as the observed annual maxima. The maxima are then compared to the sampling confidence interval from the estimated distribution to assess whether they could be likely samples. Following the method suggested in Marra et al. (2019), we select the 75<sup>th</sup> percentile of the ordinary events for the left-censoring. This is in line with previous findings in areas dominated by convective processes (Marra et al., 2019; Marra et al., 2020). It should be recalled that the selection method implies a low sensitivity of the results to this threshold.

## 2.4 Extreme value model

The cumulative distribution  $\zeta(x)$  of extreme return levels  $x$  emerging from the underlying distribution of ordinary events with tail  $F(x; \lambda, \kappa)$  can be written as  $\zeta(x) = F(x; \lambda, \kappa)^n$ , where  $n$  is the average number of ordinary events per year (Marra et al., 2019; Serinaldi et al., 2020). When one considers the  $j$ -th year of data, this formalism allows us to quantify return levels from individual years by inverting  $\zeta_j(x) = F(x; \lambda_j, \kappa_j)^{n_j}$ , where  $\lambda_j$  and  $\kappa_j$  are the parameters describing the ordinary events tail at the  $j$ -th year and  $n_j$  is the number of ordinary events in the year.

The parameters describing the ordinary events distribution tail are computed at each station, duration and year by left-censoring the lowest 75% of the ordinary events and using the least-squares method in Weibull-transformed coordinates (Marani and Ignaccolo, 2015). After left-censoring, an average of ~14 ordinary events per year (including annual maxima) are used for parameter estimation. Yearly return levels are obtained by inverting the equation for  $\zeta_j(x)$ . In this way, we obtain, for each station, yearly series of scale parameter, shape parameter, number of ordinary events, and return levels. Annual maxima (AM) series are also extracted.

## 2.5 Temporal trends analysis

We investigate the presence of monotonic trends in these quantities using the Regional Mann-Kendall test at the 0.05 significance level (Mann, 1945; Kendall, 1975; Helsel & Frans, 2006), and we quantify the average rate of change using the nonparametric Sen’s slope estimator (Sen, 1968). Serial correlation in the series was tested and found negligible. In case trends within the region are heterogeneous, the slope and significance

estimated by the Regional Mann-Kendall test could be misleading (Gilbert, 1987). We verify the homogeneity of the trends at the different sites in the area by applying the Van Belle and Hughes test (1984). We find that homogeneity is verified for all the investigated variables. As spatial correlation among nearby stations could decrease the power of regional test, we include the correction proposed by Hirsch and Slack (1984).

If the null hypothesis of the Mann-Kendall test is true (i.e., no trend) about half of the pair comparisons between ordered data points is concordant and half discordant. . Considering that 2 yr return levels correspond to the theoretical median of the AM, we consider the estimated trend on the 2 yr return levels as our model quantification of the trend in the AM.

## 2.6 Validation of the statistical model

The ability of our statistical model to reproduce observed trends in AM is verified by accounting for stochastic uncertainty in a Monte Carlo framework. For each station  $i$ , year  $j$  and duration  $d$ ,  $n_{ijd}$  Weibull-distributed ordinary events are generated according to the distribution parameters  $\lambda_{i\theta\delta}$  and  $\kappa_{i\theta\delta}$ , and the AM are extracted. The procedure is iterated 1000 times (which was found to provide coherent estimates of the 90% confidence interval), to obtain 1000 synthetic regional sets of AM series for each duration. The Regional Mann-Kendall test is then performed on these sets to obtain 1000 slopes estimates for each duration, which provide a quantification of the stochastic uncertainty in the trends of the modelled AM. It is worth noting that this confidence interval is obtained by neglecting spatial correlation in the local exceedance probability of the events, and it is thus to be considered as a lower limit to the true confidence interval. In fact, such a correlation would cause a loss of information in the regional pooling of the trend test, inflating the stochastic uncertainty in the outcome.

## 2.7 Differential impact of ordinary events change on annual maxima changes

The relative impact of trends in the ordinary events characteristics and frequency on the emerging trend in the AM is evaluated. For each station and duration, the trends on modelled AM are computed using different combinations in which inter-annual variability in the parameters is either considered or ignored. In the latter case, the median parameter is used. We thus obtain the following cases: one case with 3 time-varying parameters (real case), 3 combinations of 2 varying and 1 constant parameter, 3 combinations of 1 varying and 2 constant parameters, and one case of 3 constant parameters (no-change). Then the Regional Mann-Kendall test is applied to the resulting series.

## 2.8 Changes in the proportion of convective-like and other types of storms

Changes in the seasonal proportions between convective-like and other event types in different seasons are explored to investigate the seasonal and physical mechanisms underlying the observed trends. Events exceeding the left-censoring threshold at any of the durations are organized by seasons. The temporal decorrelation of the rain intensity timeseries is used as a proxy for broadly distinguishing between convective-like and other types of storms. The decorrelation time (**Figure 1 b**) is taken equal to the scale parameter of the exponential fitting of the temporal autocorrelation. This is thus the time lag at which the temporal autocorrelation drops to  $e^{-1}$ . For each station and season, the yearly number of storms belonging to the two groups is calculated, and the significance and slope of the regional trend is estimated using the Regional Mann-Kendall test ( $p=0.05$ ) and the Sen's slope estimator. This shows if temporal changes in the proportion of different event types in the seasons emerged. A 2 hr threshold is found to optimally describe (that is, optimize the statistical significance) the temporal changes in our data and is therefore used as a proxy for distinguishing between convective-like (decorrelation time  $[?] \leq 2$  hr) and other event types ( $> 2$  hr). Qualitatively analogous outcomes are obtained with thresholds between 1 and 3 hr.

## 3 Results and discussion

### 3.1 Regional trends on multi-duration extremes

Slopes for the regional trends for the nine investigated durations are reported in **Figure 2 a**. Hereinafter, slopes are normalized over the median value of each variable and expressed as percent change per year. As

expected (Libertino et al., 2019), observed AM show positive trends at all durations. Statistically significant trends are observed for durations up to 6 hours and stronger increases for hourly and sub-hourly durations. The slopes estimated using the model (“modelled AM” in **Figure 2**) lie within the 90% confidence interval due to stochastic uncertainty (grey area), with the exception of the longest durations (12 and 24 h). Since at longer durations, the confidence interval is likely underestimated due to a larger correlation in the severity of the storms, this indicates that they are likely samples from our model. This means that the model well reproduces the trends in the observed AM.

The annual number of storms, uniquely defined for all durations (Marra et al., 2020), shows an increase ( $0.4\% \text{ yr}^{-1}$ ) (**Figure 2 b**). Trends in the scale parameter of the intensity distributions are always positive, indicating a general increase in the intensity of the largest 25% of the ordinary events, with larger and significant increases (up to  $1.0\% \text{ yr}^{-1}$ ) for multi-hour durations (**Figure 2 b**). The shape parameter shows negative trends for sub-hourly durations and positive trends for longer durations (**Figure 2 b**), indicating that the proportion between heavy and mild events changed in different ways for short and long durations: increased tail heaviness is reported for sub-hourly durations and decreased tail heaviness for multi-hour durations (see Figure S1 for a visual interpretation of the effect of the shape parameter on tail-heaviness). At short durations the changes in the two parameters have a synergistic impact on extremes. Although the trend in individual parameters is not significant, observed and modelled AM experience stronger and significant changes. In contrast, at longer durations the changes in the parameters have opposing impact on extremes, and AM exhibit weaker increases, despite the increase of both scale parameter (significant) and yearly number of storms. In particular, where tail-heaviness has its strongest decrease (increase in the shape parameter), trends in extremes are at a minimum and are not significant.

These findings indicate that in the examined period (1991-2020) and area, AM exhibit significant changes, in particular for short-duration intensities, in agreement with previous studies (Libertino et al., 2019). Overall, our statistical model reproduces these trends accurately, and allows us to investigate the underlying statistical mechanisms. Changes in AM seem to be mostly influenced by changes in the tail-heaviness of the ordinary events, although trends in the shape parameter itself are not statistically significant.

### 3.2 Differential impact of ordinary events change on annual maxima changes

We investigate the impact of the trends in the individual model parameters on the trends in AM (**Figure 2 c**). The ‘real’ case in which all parameters change with time reproduces the trends in the modelled AM (line 1 in **Figure 2 c**). The other lines are a combination of varying and constant (median) parameters. Notably, the increase ( $+0.4\% \text{ yr}^{-1}$ ) in the number of yearly storms only has a marginal impact on the overall trends in extremes (same-color pairs of lines). Synergistic and opposing impacts of the other parameters are mostly evident by comparing the constant scale-parameter case (line 2) with the constant tail-heaviness case (line 3). When no changes in tail-heaviness are considered, AM show increasing trends whose magnitude can even increase with duration, instead of decrease (lines 3, 7). This analysis shows that little changes in the tail-heaviness (shape parameter) turn into large changes in extreme intensities, suggesting this is an important parameter explaining the observed AM trends in the region. Crucially, without considering changes in tail heaviness it is not possible to explain the large observed increase in short-duration AM, as well as the different response of short and long duration extremes. This has profound implications for change-permitting extreme value models in which tail heaviness is often assumed to remain constant.

### 3.3 Regional trends of extreme return levels

Our statistical model allows to directly quantify changes on specific rare return levels. In general, slopes are always significantly positive for sub-hourly durations and decrease with increasing duration until they lose significance for durations above 2-3 hr (**Figure 2 d**). For higher return levels, this behavior is enhanced: higher positive slopes are estimated for sub-hourly durations and lower not significant slopes for multi-hour durations. There is a duration interval between 1 and 2 hr where the trends don’t depend on return period, closely following the change in regime in which the trend in the shape parameter crosses zero, that is no change in tail heaviness.

The here adopted statistical framework gives the opportunity to quantify and evaluate the statistical significance of trends in rare return levels of interest for hydrological design and risk management. It could be argued that estimating rare return levels on a yearly basis should lead to unberable uncertainties. We showed here that the statistical significance of trends in yearly-modelled return levels as high as the 50 yr events is comparable to the statistical significance of trends in AM, suggesting a similar signal to noise ratio. Trends on extreme return levels estimated on yearly basis from our model are thus characterized by stochastic uncertainties comparable to the ones of AM.

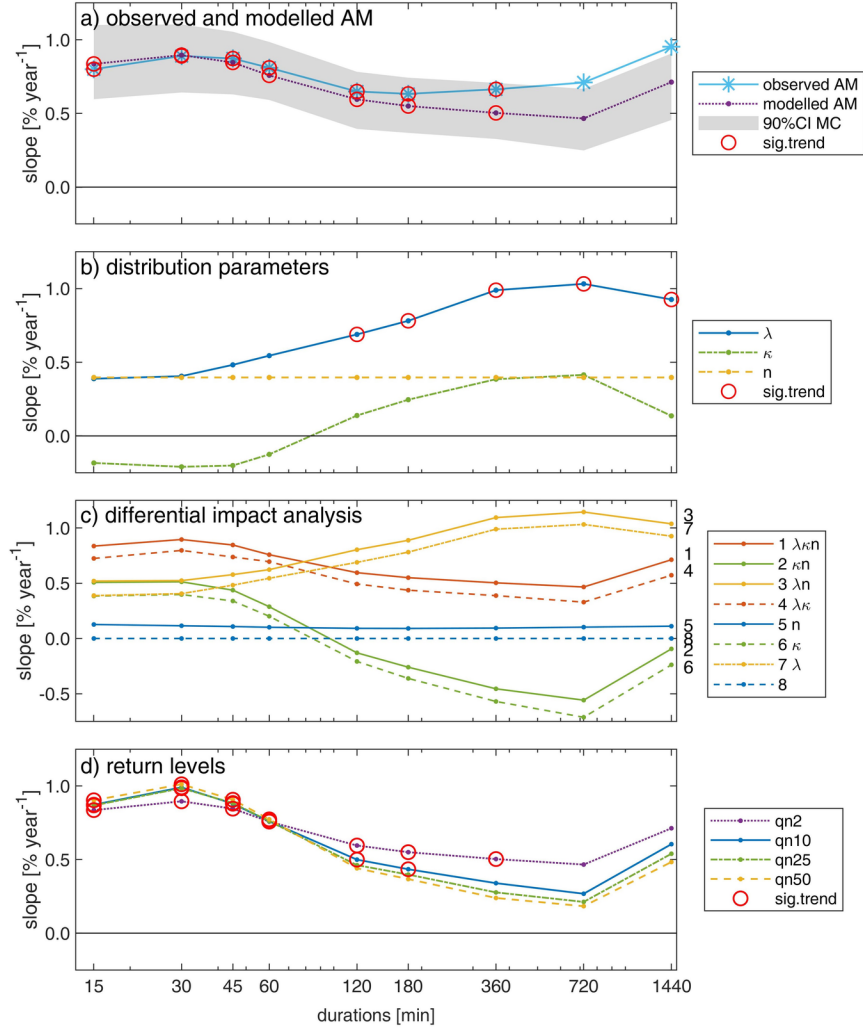


**Figure 2.** **a)** Slopes of the regional trends at different durations for observed and modelled AM; significant trends ( $\alpha$ -level=0.05) are marked; stochastic uncertainty associated with the modelled AM (90% C.I. of the MonteCarlo simulation) is also reported. **b)** Slopes of the regional trends for the model parameters: scale parameter ( $\lambda$ ), shape parameter ( $\kappa$ ), and yearly number of storms ( $n$ ); significant trends ( $\alpha$ -level=0.05) are marked. **c)** Differential impact on the modelled trends of combinations of changes and no-changes in the model parameters; series labels report the parameters which are allowed to change. **d)** Slopes of the regional trends for some estimated return levels (2, 10, 25, 50 yr); significant trends ( $\alpha$ -level=0.05) are marked; note that the 2 yr return levels correspond to the modelled AM.

### 3.4 Changes in the proportion of convective-like events

The parametrization of our model allows us to formulate hypotheses about the physical processes underlying the detected changes. In particular, the observed changes could be explained by an increased number of intense convective events, which would mainly contribute to the short duration annual maxima. We analyze possible changes in the number of storms occurring in different seasons, and in the seasonal number of convective-like and other types of storms (**Figure 3**). The positive trend in the yearly number of storms reported above is fully explained by the increases in the number of storms in autumn (SON, **Figure 3** a) and in winter (DJF). However, examining changes in the types composition shows no distinct increase in convective-like storms during these seasons (**Figure 3** b, c).

Conversely, although no trend emerges in the number of storms in summer (JJA), the number of summer convective-like storms in this season increased significantly, while the number of other storms shows no trend (**Figure 3** b, c). This implies a significant increase in the proportion of summer convective-like events. Since convective-like storms are generally associated with heavy intensities at short durations, this change in composition could explain the observed increase in tail heaviness at short durations, and thus the observed trends on short-duration AM. This is confirmed when the parameters of the ordinary events distribution are examined considering spring-summer (MAMJJA) and autumn-winter (SONDJF) separately (**Figure S2**). These results suggest that the significant positive trends found for short-duration extremes are mostly related to changes in summer storms, and that these can be related to changes in the intensity distributions (increasing tail-heaviness) induced by an increasing proportion of heavy convective-like storms in the summer.

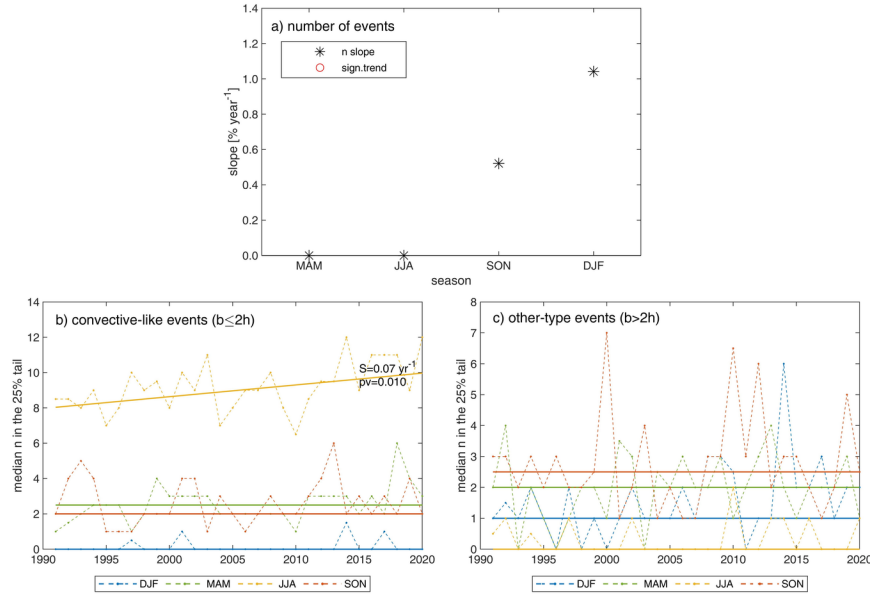


**Figure 3.** a) Slope of the regional trends for the number of seasonal storms; significant trends ( $\alpha$ -level=0.05) are marked. b) Median (across stations) seasonal number of convective-like (decorrelation time [?] 2 hr) and c) other (decorrelation time > 2 hr) storms in the 25% tail; the Sen's slope (S) and the p-value (pv) of the Regional Mann-Kendall test are reported in case of significant trends ( $\alpha$ -level=0.05).

## 5 Conclusions

We examine changes in extreme sub-daily precipitation intensities for the relevant case of the eastern Italian Alps, where consistent significant changes in annual maximum (AM) intensities were reported (Libertino et al., 2019). Specifically, we aim at detecting and quantifying trends in sub-daily AM and extreme return levels, and linking the observed trends in extremes to specific changes in the local precipitation regime. To do so, we adopt a novel unified framework for extreme value analyses based on ordinary events, and we



quantify trends by means of the regional Mann-Kendall test. With respect to traditional change-permitting extreme value models, the here presented method provides a statistical tool for better quantifying changes in extremes in spite of the large stochastic uncertainties, and for better understanding the observed changes by separately considering multi-duration storm intensity distributions and storm occurrence frequency.

Results confirm the presence of significant positive trends in the AM. Trends in the 2 yr return levels estimated yearly using our model are consistent with the observed trends in AM. These trends are more marked for 15 min to 1 hr durations and less marked for 3 hr to 24 hr durations. The model parametrization allows to conclude that these trends are likely due to a combination of (i) increasing number of storm events per year and increasing intensity of the storms, and (ii) changes in the tail properties of the storms. In particular, an increasing, albeit not-significant, trend in tail heaviness at short durations seems to mostly explain the changes in AM and return levels. A significant increase in the proportion of convective-like storms is detected during the summer (JJA). This could explain the observed trends in AM and return levels emerged at the short durations in this study. This agrees with results reported by Fowler et al. (2021a), who highlight that the stronger increases in short-duration extremes are related to feedbacks in convective clouds dynamics at the local scale. The approach can be expanded to directly consider different types of storm events (Marra et al., 2019), following previous works regarding mixed distributions like the Two-component Extreme value distribution (Rossi et al., 1984) or the mixed Gumbel (Kjeldsen et al., 2018).

The trends in this study are derived from a relatively short data series and should be considered as representative of the examined period only (1991-2020). Due to decadal climate variability, they should not be considered as representative of climate change in general, nor extrapolated to predict future conditions (Iliopoulou and Koutsoyiannis, 2020). Nevertheless, our approach could provide insights for better describing local climatologies under change, and for enhancing our understanding of the linkages with changes in the underlying physical processes. This information can be valuable for improving our ability to create and use process-based change-permitting statistical models for hydrometeorological extremes.

#### Data Availability Statement

Precipitation data was provided by the Provincia Autonoma di Trento and can be retrieved from <https://www.meteotrentino.it> (Last accessed: September 2021). The codes used for the statistical model are available at <https://doi.org/10.5281/zenodo.3971558>. The Regional Mann-Kendall trend test was performed based on the functions by J. Burkey, downloaded from <https://it.mathworks.com/matlabcentral/fileexchange/22389-seasonal-kendall-test-with-slope-for-serial-dependent-data> (retrieved July 2021). The codes developed in the study and the elaborated data for reproducing the results of the paper are available at <https://www.dropbox.com/sh/f7cf93racbg5hqv/AADXBHHTKebd5OtG9syKrIJOa?dl=0> for the purpose of peer review and, upon acceptance, will be made publicly available in their final version.

#### CRediT authors' contribution

**ED** : Data curation, Methodology, Formal analysis, Investigation, Visualization, Writing – original draft, Writing – review & editing. **MB** : Conceptualization, Investigation, Writing – review & editing, Supervision. **MZ** : Visualization, Writing – review & editing. **FM** : Conceptualization, Methodology, Software, Investigation, Writing – original draft, Writing – review & editing, Supervision.

#### Acknowledgements

The authors declare no conflict of interests. This study was funded by Provincia Autonoma di Trento through Accordo di Programma GPR. FM thanks the Institute of Atmospheric Sciences and Climate (ISAC), National Research Council of Italy for the support.

#### References

Alexander, L. V., N. Tapper, X. Zhang, H. J. Fowler, C. Tebaldi, and A. Lynch (2009), Climate extremes: Progress and future directions, *Int. J. Climatol.*, 29, 317–319.

Allan, R. P., Soden, B. J., 2008. Atmospheric Warming and the Amplification of Precipitation Extremes. *Science*, 321, 5895, 1481-1484. <https://doi.org/10.1126/science.1160787>

Blanchet J., Creutin JD., Blanc A. (2021). Retreating winter and strengthening autumn Mediterranean influence on extreme precipitation in the Southwestern Alps over the last 60 years. *Environ. Res. Lett.* 16 034056, <https://doi.org/10.1088/1748-9326/abb5cd>

Borga M., Vezzani C. & Fontana G.D. (2005). Regional Rainfall Depth–Duration–Frequency Equations for an Alpine Region. *Nat Hazards* 36, 221–235. <https://doi.org/10.1007/s11069-004-4550-y>

Chen Y., Paschalis A., Kendon E., Kim D., Onof C. (2021). Changing spatial structure of summer heavy rainfall, using convection-permitting ensemble. *Geophysical Research Letters*, 48, e2020GL090903. <https://doi.org/10.1029/2020GL090903>

Chow, V. T., Maidment, D. R., & Mays, L. W. (1988). *Applied hydrology*. McGraw-Hill

Cristiano, E., ten Veldhuis, M.-C., and van de Giesen, N. (2017). Spatial and temporal variability of rainfall and their effects on hydrological response in urban areas – a review, *Hydrol. Earth Syst. Sci.*, 21, 3859–3878, <https://doi.org/10.5194/hess-21-3859-2017>

Fatichi, S., Ivanov, V. Y., Paschalis, A., Peleg, N., Molnar, P., Rimkus, S., et al. (2016). Uncertainty partition challenges the predictability of vital details of climate change. *Earth’s Future*, 4, 240–251. <https://doi.org/10.1002/2015EF000336>

Fischer RA, Tippett LHC. (1928). Limiting forms of the frequency distribution of the largest or smallest member of a sample. *Math Proc Camb Philos Soc* 1928;24(02):180–90.

Fowler H.J., Lenderink G., Prein, A.F. et al. (2021a) Anthropogenic intensification of short-duration rainfall extremes. *Nat Rev Earth Environ* 2, 107–122. <https://doi.org/10.1038/s43017-020-00128-6>

Fowler H. J., et al. (2021b). Towards advancing scientific knowledge of climate change impacts on short-duration rainfall extremes. *Phil. Trans. R. Soc. A* 379: 20190542. <https://doi.org/10.1098/rsta.2019.0542>

Gilbert, R. O. (1987). *Statistical methods for environmental pollution monitoring*. New York City: Wiley. <https://doi.org/10.2307/1270090>

Gnedenko B. (1943). Sur la distribution limite du terme maximum d’une serie aleatoire. *Ann Math* 1943;44(3):423–53.

Groisman P.Ya., Knight R.W., Easterling D.R., Karl T.R., Hegerl G.C., Razuvaev V.N. (2005). Trends in intense precipitation in the climate record. (2005) *Journal of Climate*, 18 (9), pp. 1326-1350. Cited 935 times. doi: 10.1175/JCLI3339.1

Guerreiro, S.B., Fowler, H.J., Barbero, R. et al. (2018). Detection of continental-scale intensification of hourly rainfall extremes. *Nature Clim Change* 8, 803–807. <https://doi.org/10.1038/s41558-018-0245-3>

Haerter, J. O., P. Berg, and S. Hagemann (2010), Heavy rain intensity distributions on varying time scales and at different temperatures, *J. Geophys. Res.*, 115, D17102, doi:10.1029/2009JD013384

Helsel, D. R., & Frans, L. M. (2006). Regional Kendall test for trend. *Environmental Science & Technology*, 40(13), 4066–4073.

Hirsch, R. M.; Slack, J. R. (1984). A nonparametric trend test for seasonal data with serial dependence. *Water Resour. Res.* 1984, 20, 727-732

Iliopoulou T, Koutsoyiannis D. (2020). Projecting the future of rainfall extremes: Better classic than trendy. *J. Hydrol.*, 588 , p. 125005, <https://doi.org/10.1016/j.jhydrol.2020.125005>.

Kendall, M. G. (1975). *Rank Correlation Methods*. New York, NY: Oxford University Press.

Kjeldsen, T. R., Ahn, H., Prosdocimi I., Heo J. (2018) Mixture Gumbel models for extreme series including infrequent phenomena, *Hydrological Sciences Journal*, 63:13-14, 1927-1940, DOI: 10.1080/02626667.2018.1546956

Lenderink, G., and E. van Meijgaard (2008), Increase in hourly precipitation extremes beyond expectations from temperature changes, *Nat. Geosci.*, 1, 511–514.

Libertino A., Ganora D., & Claps P. (2019). Evidence for increasing rainfall extremes remains elusive at large spatial scales: The case of Italy. *Geophysical Research Letters*, 46, 7437–7446. <https://doi.org/10.1029/2019GL083371>

Mann, H. B. (1954) Non-parametric tests against trend. *Econometrica* 1945, 13, 245-259.

Marani M., Ignaccolo M. (2015). A metastatistical approach to rainfall extremes, *Advances in Water Resources*, Volume 79, 2015, Pages 121-126, ISSN 0309-1708, <https://doi.org/10.1016/j.advwatres.2015.03.001>.

Marchi L., Borga M., Preciso E., Gaume E. (2010). Characterisation of selected extreme flash floods in Europe and implications for flood risk management. *J. Hydrol.*, 394, pp. 118-133, <https://doi.org/10.1016/j.jhydrol.2010.07.017>

Markonis, Y., Papalexiou, S. M., Martinkova, M., & Hanel, M. (2019). Assessment of water cycle intensification over land using a multi source global gridded precipitation dataset. *Journal of Geophysical Research: Atmospheres*, <https://doi.org/10.1029/2019JD030855>

Marra, F., Armon, M., Adam, O., Zocatelli, D., Gazal, O., Garfinkel, C. I., et al. (2021). Towards narrowing uncertainty in future projections of local extreme precipitation. *Geophysical Research Letters*, 48, e2020GL091823. <https://doi.org/10.1029/2020GL091823>

Marra, F., Nikolopoulos, E. I., Anagnostou, E. N., & Morin, E. (2018). Metastatistical extreme value analysis of hourly rainfall from short records: Estimation of high quantiles and impact of measurement errors. *Advances in Water Resources*, 117, 27–39. <https://doi.org/10.1016/j.advwatres.2018.05.001>

Marra, F., Zocatelli, D., Armon, M., & Morin, E. (2019). A simplified MEV formulation to model extremes emerging from multiple nonstationary underlying processes. *Advances in Water Resources*, 127, 280–290. <https://doi.org/10.1016/j.advwatres.2019.04.002>

Marra, F., Borga, M., & Morin, E. (2020). A unified framework for extreme subdaily precipitation frequency analyses based on ordinary events. *Geophysical Research Letters*, 47, e2020GL090209.

Min SK, Zhang X, Zwiers F, Friederichs P, Hense A (2009) Signal detectability in extreme precipitation changes assessed from twentieth century climate simulations. *Clim Dyn* 32:95–111

Miniussi, A., & Marani, M. (2020). Estimation of daily rainfall extremes through the metastatistical extreme value distribution: Uncertainty minimization and implications for trend detection. *Water Resources Research*, 56, e2019WR026535. <https://doi.org/10.1029/2019WR026535>

Miniussi, A., Villarini, G., & Marani, M. (2020). Analyses through the metastatistical extreme value distribution identify contributions of tropical cyclones to rainfall extremes in the eastern United States. *Geophysical Research Letters*, 47, e2020GL087238. <https://doi.org/10.1029/2020GL087238>

Moustakis, Y., Papalexiou, S. M., Onof, C. J., & Paschalis, A. (2021). Seasonality, intensity, and duration of rainfall extremes change in a warmer climate. *Earth's Future*, 9, e2020EF001824. <https://doi.org/10.1029/2020EF001824>

Myhre, G., Alterskjær, K., Stjern, C.W. et al. Frequency of extreme precipitation increases extensively with event rareness under global warming. *Sci Rep* 9, 16063 (2019). <https://doi.org/10.1038/s41598-019-52277-4>

Papalexiou, S. M., AghaKouchak, A., & Foufoula-Georgiou, E. (2018). A diagnostic framework for understanding climatology of tails of hourly precipitation extremes in the United States. *Water Resources Research*,

54(9), 6725–6738. <https://doi.org/10.1029/2018WR022732>

Papalexiou, S. M., & Montanari, A. (2019). Global and regional increase of precipitation extremes under global warming. *Water Resources Research*, 55, 4901–4914. <https://doi.org/10.1029/2018WR024067>

Paprotny, D., Sebastian, A., Morales-Napoles, O., & Jonkman, S. N. (2018). Trends in flood losses in Europe over the past 150 years. *Nature Communications*, 9, 1985

Pendergrass, A. G. (2018). What precipitation is extreme? *Science*, 360, 6393. <https://doi.org/10.1126/science.aat1871>

Pendergrass, A.G. (2020). Changing Degree of Convective Organization as a Mechanism for Dynamic Changes in Extreme Precipitation. *Curr Clim Change Rep* 6, 47–54. <https://doi.org/10.1007/s40641-020-00157-9>

Pendergrass, A. G., Hartman, D. L. (2014). The Atmospheric Energy Constraint on Global-Mean Precipitation Change. *J. Climate*, 27, 2, 757–768, <https://doi.org/10.1175/JCLI-D-13-00163.1>

Prosdocimi, I., Kjeldsen, T. Parametrisation of change-permitting extreme value models and its impact on the description of change. *Stoch Environ Res Risk Assess* 35, 307–324 (2021). <https://doi.org/10.1007/s00477-020-01940-8>

Rossi, F., Fiorentino, M., and Versace, P. (1984), Two-Component Extreme Value Distribution for Flood Frequency Analysis, *Water Resour. Res.*, 20( 7), 847– 856, doi:10.1029/WR020i007p00847.

Schär C., N. Ban, E.M. Fischer, et al., 2016. Percentile indices for assessing changes in heavy precipitation events. *Clim. Change*, 137, 201–216, <https://doi.org/10.1007/s10584-016-1669-2>

Sen PK (1968). Estimates of the regression coefficient based on Kendall’s tau, *J. Am. Statist. Assoc.*, 63, 1379–1389, <http://doi.org/10.1080/01621459.1968.10480934>

Serinaldi, F., & Kilsby, C. G. (2015). Stationarity is undead: Uncertainty dominates the distribution of extremes. *Advances in Water Resources*, 77, 17–36.

Trenberth, K. E., A. Dai, R. M. Rasmussen, and D. B. Parsons (2003), The changing character of precipitation, *Bull. Am. Meteorol. Soc.*, 84, 1205– 1217.

van Belle G., Hughes, J. P. (1984) Nonparametric tests for trend in water quality. *Water Resour. Res.* 1984, 20, 127–136.

Zheng F., Westra S., Leonard M. (2015). Opposing local precipitation extremes. *Nature Clim Change* 5, 389–390. <https://doi.org/10.1038/nclimate2579>

Zorzetto E., Botter G., Marani M. (2016). On the emergence of rainfall extremes from ordinary events. *Geophysical Research Letters*, 43, 8076–8082. <https://doi.org/10.1002/2016GL069445>

**Enhanced summer convection explains observed trends in extreme subdaily precipitation in the northeastern Italian Alps**

**E. Dallan<sup>1</sup>, M. Borga<sup>1</sup>, M. Zaramella<sup>1</sup>, F. Marra<sup>2</sup>**

<sup>1</sup>Department of Land Environment Agriculture and Forestry, University of Padova, Padova, Italy

<sup>2</sup> National Research Council of Italy - Institute of Atmospheric Sciences and Climate (CNR-ISAC), Bologna, Italy

Corresponding author: Eleonora Dallan ([eleonora.dallan@unipd.it](mailto:eleonora.dallan@unipd.it))

**Key Points:**

- We present a method for analyzing extreme precipitation trends based on the separation of storm intensity and occurrence frequency
- Our approach reproduces observed trends in annual maxima and allows to quantify trends on rare return levels
- Observed trends in the eastern Italian Alps are explained by an increased proportion of heavy convective storms in the summer

## Abstract

Understanding past changes in precipitation extremes could help us predict their dynamics under future conditions. We present a novel approach for analyzing trends in extremes and attributing them to changes in the local precipitation regime. The approach relies on the separation between intensity distribution and occurrence frequency of storms. We examine the relevant case of the eastern Italian Alps, where significant trends in annual maximum precipitation over the past decades were observed. The model is able to reproduce observed trends at all durations between 15 minutes and 24 hours, and allows to quantify trends in extreme return levels. Despite the significant increase in storms occurrence and typical intensity, the observed trends can be only explained considering changes in the tail heaviness of the intensity distribution, that is the proportion between heavy and mild events. Our results suggest these are caused by an increased proportion of summer convective storms.

## Plain Language Summary

Quantifying past trends in extreme rainfall is important because it can help us understand future changes caused by global warming. Climate scientists and hydrologists use specific statistical models to do so, but interpreting the results is complicated because extremes are rare and the structure of the models is not linked to the local meteorology. We use a new statistical model that allows to better understand the mechanisms behind the trends we detect. We find that extreme rainfall in the eastern Italian Alps increased over the past decades and we associate this change to an increased proportion of summer thunderstorms.

## 1 Introduction

Understanding past and future changes in extreme subdaily precipitation intensities is of enormous interest because they are responsible for flash floods, urban floods, landslides and debris flows, and cause numerous casualties and huge damages every year (Borga et al., 2014; Cristiano et al., 2017; Paprotny et al., 2018). Physical laws translate increasing atmospheric temperature into increasing water vapor holding capacity. Together with changes in the atmospheric dynamics, this is expected to drive future precipitation changes (Trenberth et al., 2003; Pendergrass et al., 2020; Fowler et al., 2021b). In general, larger responses are expected for precipitation extremes because mean precipitation, on a global scale, is limited by energy constraints (Allan and Soden, 2008; Pendergrass & Hartmann, 2014). However, detecting changes in extreme precipitation is highly affected by the stochastic uncertainty characterizing the sampling of extremes. This uncertainty may mask the influence of climate forcing on the processes which locally control the extremes (Fatichi et al., 2016; Marra et al., 2019).

Statistically significant changes in the frequency of extreme precipitation in the past decades were reported, often with stronger trends in subdaily extremes, as opposed to daily (Guerreiro et al., 2018; Markonis et al., 2019; Papalexiou & Montanari, 2019). In some cases, opposing trends between short and long durations emerged, with complex implications for flood risk (Zheng et al., 2015). Available observations show different temporal trends for precipitation intensities associated to different exceedance probabilities (Schär et al., 2016; Pendergrass, 2018). In general, increasing trends are reported for rarer events (Myhre et al., 2019), but the specific differences depend on duration, season, and local conditions, such as the dominating meteorological features contributing extremes (Blanchet et al., 2021; Moustakis et al., 2021).

Extreme return levels characterized by different exceedance probabilities are thus changing at different rates (Myhre et al., 2019; Marra et al., 2021).

Nonstationary extreme value models could aid the detection and quantification of trends in extreme precipitation of different exceedance probability (e.g., Min et al. 2009). However, the information these models can provide is impacted by stochastic uncertainties (Serinaldi and Kilsby, 2015; Fatichi et al., 2016), and their flexibility is limited by the assumptions concerning high order statistical moments. In fact, due to intrinsic limitations in parameter estimation accuracy, the shape (and sometimes also the scale) parameter of the extreme value distribution is usually assumed to be constant (Prosdocimi and Kjeldsen, 2021). Additionally, due to the structure of these statistical models, a link between the properties of the underlying process, such as precipitation occurrence frequency and intensity distribution, and extremes is difficult to establish (e.g. Marra et al., 2019). As such, the possibility to attribute the observed changes to specific physical and meteorological processes is hampered.

This background suggests that there is a need to move beyond traditional trend detection techniques applied to extremes only and develop novel methodologies. These methods should be able to detect general changes in extreme precipitation at multiple durations, quantify changes at different exceedance probabilities, and attribute these to changes in the underlying physical processes.

Miniussi and Marani (2020) proposed the so-called Metastatistical Extreme Value approach (Marani and Ignaccolo, 2015) as a viable way for addressing these issues. The idea relies on the concept of *ordinary events*, that is all the independent realizations of a process of interest, and proved highly effective in reducing stochasting uncertainties (Zorzetto et al., 2016; Marra et al., 2018). As opposed to traditional methods, the distribution describing the ordinary events is assumed to be known, and the extreme value distribution is derived by explicitly considering the occurrence frequency of the ordinary events. Miniussi and Marani (2020) provided an example application in which extreme return levels were computed over moving time windows, highlighting temporal changes that could not be appreciated using traditional methods. The adopted ordinary events (daily precipitation amounts), however, were not directly connected with meteorological systems, so that direct relations between changes in extremes and changes in the underlying storm properties is still missing.

Here, we combine a novel approach for ordinary-events-based precipitation frequency analyses across durations (Marra et al., 2020) with a regional trend detection technique to: (a) detect and quantify trends in sub-daily annual maxima and extreme return levels by independently considering the changes in properties and occurrence frequency of storms, and (b) attribute the observed trends in extremes to specific changes in the local precipitation regime. We examine the relevant case of the eastern Italian Alps, where consistent significant changes in annual maximum precipitation intensities at subdaily and daily duration were reported (Libertino et al., 2019).

## 2 Data and methodology

### 2.1 Study area and data

We focus on Trentino, a 6000 km<sup>2</sup>-wide mountainous area in the Eastern Italian Alps (**Figure 1a**) which experienced significant increases in extreme short-duration rain intensities over the last decades (Libertino et al., 2019). Mean annual precipitation varies from ~1300 mm

yr<sup>-1</sup> in the south-eastern portion of the area to lower amounts (~900 mm yr<sup>-1</sup>) typical of the “inner alpine province” in the north (Borga et al., 2005). A dense network of more than one hundred rain gauges is present. From these, 30 stations (density ~1/200 km<sup>-2</sup>) with at least 27 complete years (<10% missing data) of 5-minute resolution data in the period 1991-2020 are selected (Figure 1a; see Table S1 in the Supporting Information).

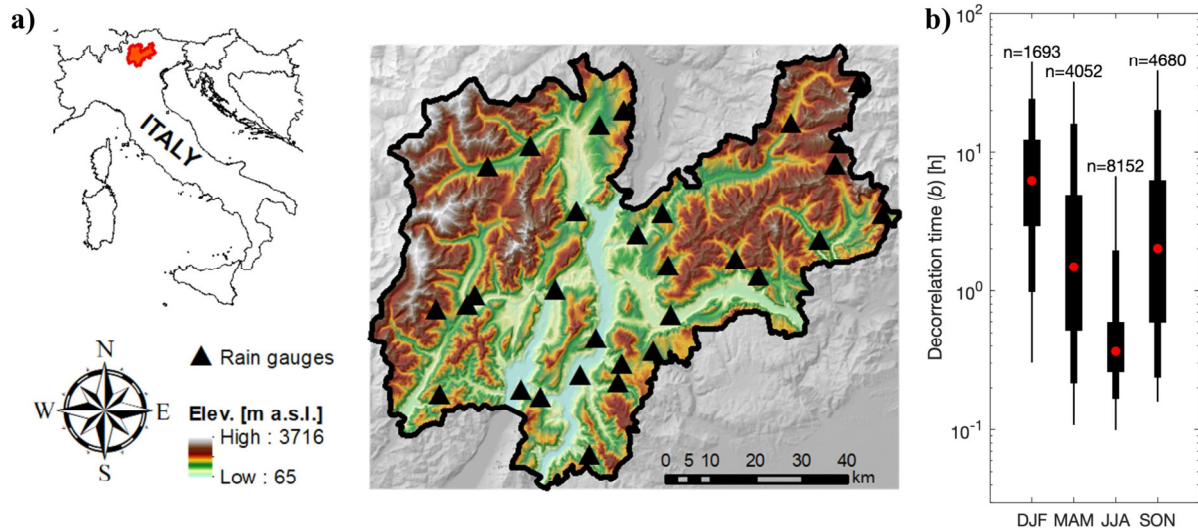


**Figure 1. a)** Location and orography of the study area and location of the rain gauges used in this study; **b)** Decorrelation time of the highest 25% ordinary events organized by season. The red dots indicate the median values; bars indicate percentiles: 25-75th, 5-95th, 1-99th. The number of storms occurred across the stations in each season is reported.

## 2.2 Definition of the ordinary events

Ordinary events are all the independent realizations of a process of interest, in our case precipitation intensities at multiple durations. The here presented analysis is based on the storm-based identification of ordinary events proposed by Marra et al. (2020), in which “storms” are defined as independent meteorological objects, and “ordinary events” of each duration are extracted from the storms. For each station, storms are defined as wet periods separated by dry hiatuses of predefined length. We define as wet all the 5 min time intervals reporting at least 0.1 mm of precipitation, and separate storms using 24 hr dry hiatuses. A minimum duration of 30 min for a single storm is set to avoid individual tips to be considered as storms. Ordinary events are then defined as the maximum intensities observed over the duration of interest in each storm (details in Marra et al., 2020). Durations between 15 min to 24 hr are explored: 15 min, 30 min, 45 min, 1 h, 2 h, 3 h, 6 h, 12 h, 24h.

## 2.3 Tail of the ordinary events distribution

Previous studies show that subdaily precipitation intensities require three- (or more) parameters distributions (Papalexiou et al., 2018). However, their right tails can be well approximated using a two-parameter distribution which, in many cases, is found to be a Weibull distribution (e.g., Zorzetto et al. 2016; Marra et al., 2020). This means that a portion of their distribution including the extremes, which is here termed “tail”, can be approximated



as  $F(x; \lambda, \kappa) = 1 - e^{-\left(\frac{x}{\lambda}\right)^\kappa}$ , where  $\lambda$  is a scale parameter and  $\kappa$  is a shape parameter which determines the tail heaviness. Larger shape parameters are associated to lighter tails, and vice versa (see Figure S1). In particular, the tail is sub-exponential for  $\kappa > 1$ , exponential for  $\kappa=1$ , and heavier than exponential for  $\kappa < 1$ .

The choice of the left-censoring threshold follows the test described in Marra et al. (2020): the distribution parameters are estimated for different thresholds by censoring the values below the left-censoring threshold as well as the observed annual maxima. The maxima are then compared to the sampling confidence interval from the estimated distribution to assess whether they could be likely samples. Following the method suggested in Marra et al. (2019), we select the 75<sup>th</sup> percentile of the ordinary events for the left-censoring. This is in line with previous findings in areas dominated by convective processes (Marra et al., 2019; Marra et al., 2020). It should be recalled that the selection method implies a low sensitivity of the results to this threshold.

## 2.4 Extreme value model

The cumulative distribution  $\zeta(x)$  of extreme return levels  $x$  emerging from the underlying distribution of ordinary events with tail  $F(x; \lambda, \kappa)$  can be written as  $\zeta(x) = F(x; \lambda, \kappa)^n$ , where  $n$  is the average number of ordinary events per year (Marra et al., 2019; Serinaldi et al., 2020). When one considers the  $j$ -th year of data, this formalism allows us to quantify return levels from individual years by inverting  $\zeta_j(x) = F(x; \lambda_j, \kappa_j)^{n_j}$ , where  $\lambda_j$  and  $\kappa_j$  are the parameters describing the ordinary events tail at the  $j$ -th year and  $n_j$  is the number of ordinary events in the year.

The parameters describing the ordinary events distribution tail are computed at each station, duration and year by left-censoring the lowest 75% of the ordinary events and using the least-squares method in Weibull-transformed coordinates (Marani and Ignaccolo, 2015). After left-censoring, an average of  $\sim 14$  ordinary events per year (including annual maxima) are used for parameter estimation. Yearly return levels are obtained by inverting the equation for  $\zeta_j(x)$ . In this way, we obtain, for each station, yearly series of scale parameter, shape parameter, number of ordinary events, and return levels. Annual maxima (AM) series are also extracted.

## 2.5 Temporal trends analysis

We investigate the presence of monotonic trends in these quantities using the Regional Mann-Kendall test at the 0.05 significance level (Mann, 1945; Kendall, 1975; Helsel & Frans, 2006), and we quantify the average rate of change using the nonparametric Sen's slope estimator (Sen, 1968). Serial correlation in the series was tested and found negligible. In case trends within the region are heterogeneous, the slope and significance estimated by the Regional Mann-Kendall test could be misleading (Gilbert, 1987). We verify the homogeneity of the trends at the different sites in the area by applying the Van Belle and Hughes test (1984). We find that homogeneity is verified for all the investigated variables. As spatial correlation among nearby stations could decrease the power of regional test, we include the correction proposed by Hirsch and Slack (1984).

If the null hypothesis of the Mann-Kendall test is true (i.e., no trend) about half of the pair comparisons between ordered data points is concordant and half discordant. . Considering

that 2 yr return levels correspond to the theoretical median of the AM, we consider the estimated trend on the 2 yr return levels as our model quantification of the trend in the AM.

## 2.6 Validation of the statistical model

The ability of our statistical model to reproduce observed trends in AM is verified by accounting for stochastic uncertainty in a Monte Carlo framework. For each station  $i$ , year  $j$  and duration  $d$ ,  $n_{ijd}$  Weibull-distributed ordinary events are generated according to the distribution parameters  $\lambda_{ijd}$  and  $\kappa_{ijd}$ , and the AM are extracted. The procedure is iterated 1000 times (which was found to provide coherent estimates of the 90% confidence interval), to obtain 1000 synthetic regional sets of AM series for each duration. The Regional Mann-Kendall test is then performed on these sets to obtain 1000 slopes estimates for each duration, which provide a quantification of the stochastic uncertainty in the trends of the modelled AM. It is worth noting that this confidence interval is obtained by neglecting spatial correlation in the local exceedance probability of the events, and it is thus to be considered as a lower limit to the true confidence interval. In fact, such a correlation would cause a loss of information in the regional pooling of the trend test, inflating the stochastic uncertainty in the outcome.

## 2.7 Differential impact of ordinary events change on annual maxima changes

The relative impact of trends in the ordinary events characteristics and frequency on the emerging trend in the AM is evaluated. For each station and duration, the trends on modelled AM are computed using different combinations in which inter-annual variability in the parameters is either considered or ignored. In the latter case, the median parameter is used. We thus obtain the following cases: one case with 3 time-varying parameters (real case), 3 combinations of 2 varying and 1 constant parameter, 3 combinations of 1 varying and 2 constant parameters, and one case of 3 constant parameters (no-change). Then the Regional Mann-Kendall test is applied to the resulting series.

## 2.8 Changes in the proportion of convective-like and other types of storms

Changes in the seasonal proportions between convective-like and other event types in different seasons are explored to investigate the seasonal and physical mechanisms underlying the observed trends. Events exceeding the left-censoring threshold at any of the durations are organized by seasons. The temporal decorrelation of the rain intensity timeseries is used as a proxy for broadly distinguishing between convective-like and other types of storms. The decorrelation time (**Figure 1b**) is taken equal to the scale parameter of the exponential fitting of the temporal autocorrelation. This is thus the time lag at which the temporal autocorrelation drops to  $e^{-1}$ . For each station and season, the yearly number of storms belonging to the two groups is calculated, and the significance and slope of the regional trend is estimated using the Regional Mann-Kendall test ( $p=0.05$ ) and the Sen's slope estimator. This shows if temporal changes in the proportion of different event types in the seasons emerged. A 2 hr threshold is found to optimally describe (that is, optimize the statistical significance) the temporal changes in our data and is therefore used as a proxy for distinguishing between convective-like (decorrelation time  $\leq 2$  hr) and other event types ( $> 2$  hr). Qualitatively analogous outcomes are obtained with thresholds between 1 and 3 hr.

### 3 Results and discussion

#### 3.1 Regional trends on multi-duration extremes

Slopes for the regional trends for the nine investigated durations are reported in **Figure 2a**. Hereinafter, slopes are normalized over the median value of each variable and expressed as percent change per year. As expected (Libertino et al., 2019), observed AM show positive trends at all durations. Statistically significant trends are observed for durations up to 6 hours and stronger increases for hourly and sub-hourly durations. The slopes estimated using the model (“modelled AM” in **Figure 2**) lie within the 90% confidence interval due to stochastic uncertainty (grey area), with the exception of the longest durations (12 and 24 h). Since at longer durations, the confidence interval is likely underestimated due to a larger correlation in the severity of the storms, this indicates that they are likely samples from our model. This means that the model well reproduces the trends in the observed AM.

The annual number of storms, uniquely defined for all durations (Marra et al., 2020), shows an increase ( $0.4\% \text{ yr}^{-1}$ ) (**Figure 2b**). Trends in the scale parameter of the intensity distributions are always positive, indicating a general increase in the intensity of the largest 25% of the ordinary events, with larger and significant increases (up to  $1.0\% \text{ yr}^{-1}$ ) for multi-hour durations (**Figure 2b**). The shape parameter shows negative trends for sub-hourly durations and positive trends for longer durations (**Figure 2b**), indicating that the proportion between heavy and mild events changed in different ways for short and long durations: increased tail heaviness is reported for sub-hourly durations and decreased tail heaviness for multi-hour durations (see Figure S1 for a visual interpretation of the effect of the shape parameter on tail-heaviness). At short durations the changes in the two parameters have a synergistic impact on extremes. Although the trend in individual parameters is not significant, observed and modelled AM experience stronger and significant changes. In contrast, at longer durations the changes in the parameters have opposing impact on extremes, and AM exhibit weaker increases, despite the increase of both scale parameter (significant) and yearly number of storms. In particular, where tail-heaviness has its strongest decrease (increase in the shape parameter), trends in extremes are at a minimum and are not significant.

These findings indicate that in the examined period (1991-2020) and area, AM exhibit significant changes, in particular for short-duration intensities, in agreement with previous studies (Libertino et al., 2019). Overall, our statistical model reproduces these trends accurately, and allows us to investigate the underlying statistical mechanisms. Changes in AM seem to be mostly influenced by changes in the tail-heaviness of the ordinary events, although trends in the shape parameter itself are not statistically significant.

#### 3.2 Differential impact of ordinary events change on annual maxima changes

We investigate the impact of the trends in the individual model parameters on the trends in AM (**Figure 2c**). The ‘real’ case in which all parameters change with time reproduces the trends in the modelled AM (line 1 in **Figure 2c**). The other lines are a combination of varying and constant (median) parameters. Notably, the increase ( $+0.4\% \text{ yr}^{-1}$ ) in the number of yearly storms only has a marginal impact on the overall trends in extremes (same-color pairs of lines). Synergistic and opposing impacts of the other parameters are mostly evident by comparing the constant scale-parameter case (line 2) with the constant tail-heaviness case (line 3). When no changes in tail-heaviness are considered, AM show increasing trends whose magnitude can even

increase with duration, instead of decrease (lines 3, 7). This analysis shows that little changes in the tail-heaviness (shape parameter) turn into large changes in extreme intensities, suggesting this is an important parameter explaining the observed AM trends in the region. Crucially, without considering changes in tail heaviness it is not possible to explain the large observed increase in short-duration AM, as well as the different response of short and long duration extremes. This has profound implications for change-permitting extreme value models in which tail heaviness is often assumed to remain constant.

### 3.3 Regional trends of extreme return levels

Our statistical model allows to directly quantify changes on specific rare return levels. In general, slopes are always significantly positive for sub-hourly durations and decrease with increasing duration until they lose significance for durations above 2-3 hr (**Figure 2d**). For higher return levels, this behavior is enhanced: higher positive slopes are estimated for sub-hourly durations and lower not significant slopes for multi-hour durations. There is a duration interval between 1 and 2 hr where the trends don't depend on return period, closely following the change in regime in which the trend in the shape parameter crosses zero, that is no change in tail heaviness.

The here adopted statistical framework gives the opportunity to quantify and evaluate the statistical significance of trends in rare return levels of interest for hydrological design and risk management. It could be argued that estimating rare return levels on a yearly basis should lead to unbearable uncertainties. We showed here that the statistical significance of trends in yearly-modelled return levels as high as the 50 yr events is comparable to the statistical significance of trends in AM, suggesting a similar signal to noise ratio. Trends on extreme return levels estimated on yearly basis from our model are thus characterized by stochastic uncertainties comparable to the ones of AM.

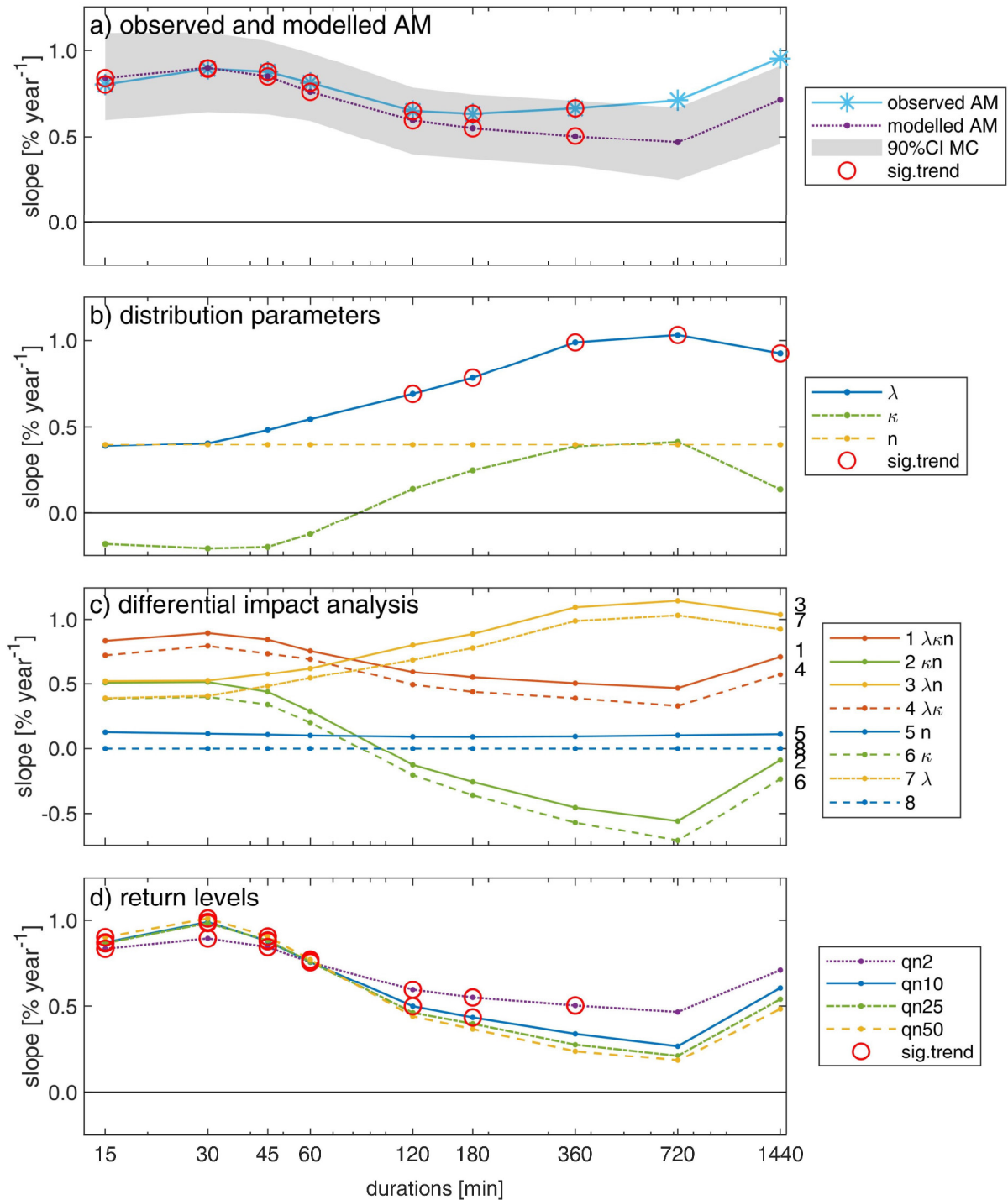


**Figure 2. a)** Slopes of the regional trends at different durations for observed and modelled AM; significant trends ( $\alpha$ -level=0.05) are marked; stochastic uncertainty associated with the modelled AM (90% C.I. of the Monte Carlo simulation) is also reported. **b)** Slopes of the regional trends for the model parameters: scale parameter ( $\lambda$ ), shape parameter ( $\kappa$ ), and yearly number of storms ( $n$ ); significant trends ( $\alpha$ -level=0.05) are marked. **c)** Differential impact on the modelled trends

of combinations of changes and no-changes in the model parameters; series labels report the parameters which are allowed to change. **d)** Slopes of the regional trends for some estimated return levels (2, 10, 25, 50 yr); significant trends ( $\alpha$ -level=0.05) are marked; note that the 2 yr return levels correspond to the modelled AM.

### 3.4 Changes in the proportion of convective-like events

The parametrization of our model allows us to formulate hypotheses about the physical processes underlying the detected changes. In particular, the observed changes could be explained by an increased number of intense convective events, which would mainly contribute to the short duration annual maxima. We analyze possible changes in the number of storms occurring in different seasons, and in the seasonal number of convective-like and other types of storms (**Figure 3**). The positive trend in the yearly number of storms reported above is fully explained by the increases in the number of storms in autumn (SON, **Figure 3a**) and in winter (DJF). However, examining changes in the types composition shows no distinct increase in convective-like storms during these seasons (**Figure 3b, c**).

Conversely, although no trend emerges in the number of storms in summer (JJA), the number of summer convective-like storms in this season increased significantly, while the number of other storms shows no trend (**Figure 3b, c**). This implies a significant increase in the proportion of summer convective-like events. Since convective-like storms are generally associated with heavy intensities at short durations, this change in composition could explain the observed increase in tail heaviness at short durations, and thus the observed trends on short-duration AM. This is confirmed when the parameters of the ordinary events distribution are examined considering spring-summer (MAMJJA) and autumn-winter (SONDJF) separately (**Figure S2**). These results suggest that the significant positive trends found for short-duration extremes are mostly related to changes in summer storms, and that these can be related to changes in the intensity distributions (increasing tail-heaviness) induced by an increasing proportion of heavy convective-like storms in the summer.

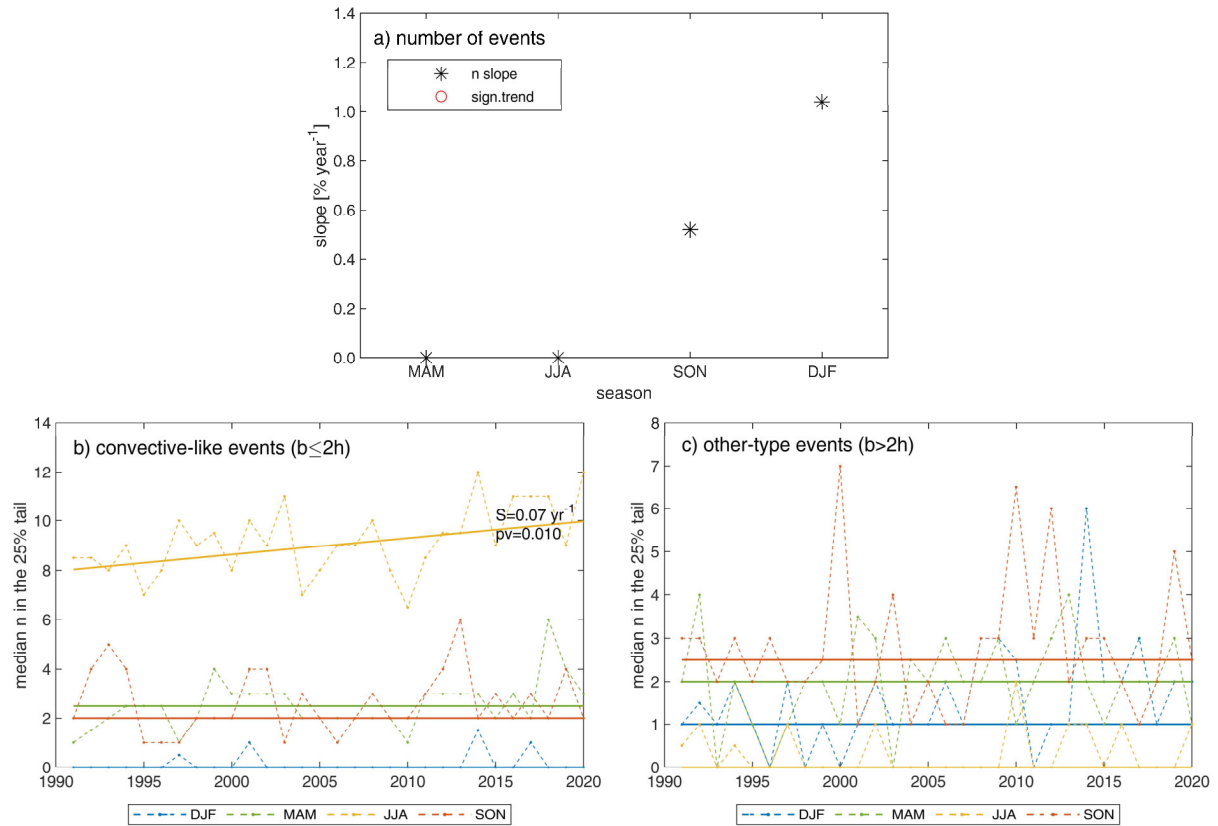


**Figure 3. a)** Slope of the regional trends for the number of seasonal storms; significant trends ( $\alpha$ -level=0.05) are marked. **b)** Median (across stations) seasonal number of convective-like (decorrelation time  $\leq 2$  hr) and **c)** other (decorrelation time  $> 2$  hr) storms in the 25% tail; the Sen's slope (S) and the p-value (pv) of the Regional Mann-Kendall test are reported in case of significant trends ( $\alpha$ -level=0.05).

## 5 Conclusions

We examine changes in extreme sub-daily precipitation intensities for the relevant case of the eastern Italian Alps, where consistent significant changes in annual maximum (AM) intensities were reported (Libertino et al., 2019). Specifically, we aim at detecting and quantifying trends in sub-daily AM and extreme return levels, and linking the observed trends in extremes to specific changes in the local precipitation regime. To do so, we adopt a novel unified framework for extreme value analyses based on ordinary events, and we quantify trends by means of the regional Mann-Kendall test. With respect to traditional change-permitting extreme value models, the here presented method provides a statistical tool for better quantifying changes in extremes in spite of the large stochastic uncertainties, and for better understanding the observed changes by separately considering multi-duration storm intensity distributions and storm occurrence frequency.

Results confirm the presence of significant positive trends in the AM. Trends in the 2 yr return levels estimated yearly using our model are consistent with the observed trends in AM. These trends are more marked for 15 min to 1 hr durations and less marked for 3 hr to 24 hr

329 durations. The model parametrization allows to conclude that these trends are likely due to a  
 330 combination of (i) increasing number of storm events per year and increasing intensity of the  
 331 storms, and (ii) changes in the tail properties of the storms. In particular, an increasing, albeit  
 332 not-significant, trend in tail heaviness at short durations seems to mostly explain the changes in  
 333 AM and return levels. A significant increase in the proportion of convective-like storms is  
 334 detected during the summer (JJA). This could explain the observed trends in AM and return  
 335 levels emerged at the short durations in this study. This agrees with results reported by Fowler et  
 336 al. (2021a), who highlight that the stronger increases in short-duration extremes are related to  
 337 feedbacks in convective clouds dynamics at the local scale. The approach can be expanded to  
 338 directly consider different types of storm events (Marra et al., 2019), following previous works  
 339 regarding mixed distributions like the Two-component Extreme value distribution (Rossi et al.,  
 340 1984) or the mixed Gumbel (Kjeldsen et al., 2018).

341 The trends in this study are derived from a relatively short data series and should be  
 342 considered as representative of the examined period only (1991-2020). Due to decadal climate  
 343 variability, they should not be considered as representative of climate change in general, nor  
 344 extrapolated to predict future conditions (Iliopoulou and Koutsoyiannis, 2020). Nevertheless,  
 345 our approach could provide insights for better describing local climatologies under change, and  
 346 for enhancing our understanding of the linkages with changes in the underlying physical  
 347 processes. This information can be valuable for improving our ability to create and use process-  
 348 based change-permitting statistical models for hydrometeorological extremes.

## 349 **Data Availability Statement**

350 Precipitation data was provided by the Provincia Autonoma di Trento and can be  
 351 retrieved from <https://www.meteotrentino.it> (Last accessed: September 2021). The codes used  
 352 for the statistical model are available at <https://doi.org/10.5281/zenodo.3971558>. The Regional  
 353 Mann-Kendall trend test was performed based on the functions by J. Burkey, downloaded from  
 354 [https://it.mathworks.com/matlabcentral/fileexchange/22389-seasonal-kendall-test-with-slope-for-](https://it.mathworks.com/matlabcentral/fileexchange/22389-seasonal-kendall-test-with-slope-for-serial-dependent-data)  
 355 [serial-dependent-data](https://it.mathworks.com/matlabcentral/fileexchange/22389-seasonal-kendall-test-with-slope-for-serial-dependent-data) (retrieved July 2021). The codes developed in the study and the elaborated  
 356 data for reproducing the results of the paper are available at  
 357 <https://www.dropbox.com/sh/f7cf93racbg5hqv/AADXBHHTKebd5OtG9syKrIJOa?dl=0> for the  
 358 purpose of peer review and, upon acceptance, will be made publicly available in their final  
 359 version.

## 360 **CRediT authors' contribution**

361 **ED:** Data curation, Methodology, Formal analysis, Investigation, Visualization, Writing –  
 362 original draft, Writing – review & editing. **MB:** Conceptualization, Investigation, Writing –  
 363 review & editing, Supervision. **MZ:** Visualization, Writing – review & editing. **FM:**  
 364 Conceptualization, Methodology, Software, Investigation, Writing – original draft, Writing –  
 365 review & editing, Supervision.

## 366 **Acknowledgements**

367 The authors declare no conflict of interests. This study was funded by Provincia  
 368 Autonoma di Trento through Accordo di Programma GPR. FM thanks the Institute of  
 369 Atmospheric Sciences and Climate (ISAC), National Research Council of Italy for the support.



## References

- Alexander, L. V., N. Tapper, X. Zhang, H. J. Fowler, C. Tebaldi, and A. Lynch (2009), Climate extremes: Progress and future directions, *Int. J. Climatol.*, 29, 317–319.
- Allan, R. P., Soden, B. J., 2008. Atmospheric Warming and the Amplification of Precipitation Extremes. *Science*, 321, 5895, 1481–1484. <https://doi.org/10.1126/science.1160787>
- Blanchet J., Creutin JD., Blanc A. (2021). Retreating winter and strengthening autumn Mediterranean influence on extreme precipitation in the Southwestern Alps over the last 60 years. *Environ. Res. Lett.* 16 034056, <https://doi.org/10.1088/1748-9326/abb5cd>
- Borga M., Vezzani C. & Fontana G.D. (2005). Regional Rainfall Depth–Duration–Frequency Equations for an Alpine Region. *Nat Hazards* 36, 221–235. <https://doi.org/10.1007/s11069-004-4550-y>
- Chen Y., Paschalis A., Kendon E., Kim D., Onof C. (2021). Changing spatial structure of summer heavy rainfall, using convection-permitting ensemble. *Geophysical Research Letters*, 48, e2020GL090903. <https://doi.org/10.1029/2020GL090903>
- Chow, V. T., Maidment, D. R., & Mays, L. W. (1988). *Applied hydrology*. McGraw-Hill
- Cristiano, E., ten Veldhuis, M.-C., and van de Giesen, N. (2017). Spatial and temporal variability of rainfall and their effects on hydrological response in urban areas – a review, *Hydrol. Earth Syst. Sci.*, 21, 3859–3878, <https://doi.org/10.5194/hess-21-3859-2017>
- Fatichi, S., Ivanov, V. Y., Paschalis, A., Peleg, N., Molnar, P., Rimkus, S., et al. (2016). Uncertainty partition challenges the predictability of vital details of climate change. *Earth's Future*, 4, 240–251. <https://doi.org/10.1002/2015EF000336>
- Fischer RA, Tippett LHC. (1928). Limiting forms of the frequency distribution of the largest or smallest member of a sample. *Math Proc Camb Philos Soc* 1928;24(02):180–90.
- Fowler H.J., Lenderink G., Prein, A.F. et al. (2021a) Anthropogenic intensification of short-duration rainfall extremes. *Nat Rev Earth Environ* 2, 107–122. <https://doi.org/10.1038/s43017-020-00128-6>
- Fowler H. J., et al. (2021b). Towards advancing scientific knowledge of climate change impacts on short-duration rainfall extremes. *Phil. Trans. R. Soc. A* 379: 20190542. <https://doi.org/10.1098/rsta.2019.0542>
- Gilbert, R. O. (1987). *Statistical methods for environmental pollution monitoring*. New York City: Wiley. <https://doi.org/10.2307/1270090>
- Gnedenko B. (1943). Sur la distribution limite du terme maximum d'une serie aleatoire. *Ann Math* 1943;44(3):423–53.
- Groisman P.Ya., Knight R.W., Easterling D.R., Karl T.R., Hegerl G.C., Razuvaev V.N. (2005). Trends in intense precipitation in the climate record. (2005) *Journal of Climate*, 18 (9), pp. 1326–1350. Cited 935 times. doi: 10.1175/JCLI3339.1
- Guerreiro, S.B., Fowler, H.J., Barbero, R. et al. (2018). Detection of continental-scale intensification of hourly rainfall extremes. *Nature Clim Change* 8, 803–807. <https://doi.org/10.1038/s41558-018-0245-3>

- Haerter, J. O., P. Berg, and S. Hagemann (2010), Heavy rain intensity distributions on varying time scales and at different temperatures, *J. Geophys. Res.*, 115, D17102, doi:10.1029/2009JD013384
- Helsel, D. R., & Frans, L. M. (2006). Regional Kendall test for trend. *Environmental Science & Technology*, 40(13), 4066–4073.
- Hirsch, R. M.; Slack, J. R. (1984). A nonparametric trend test for seasonal data with serial dependence. *Water Resour. Res.* 1984, 20, 727-732
- Iliopoulou T, Koutsoyiannis D. (2020). Projecting the future of rainfall extremes: Better classic than trendy. *J. Hydrol.*, 588 , p. 125005, <https://doi.org/10.1016/j.jhydrol.2020.125005>.
- Kendall, M. G. (1975). *Rank Correlation Methods*. New York, NY: Oxford University Press.
- Kjeldsen, T. R., Ahn, H., Prosdocimi I., Heo J. (2018) Mixture Gumbel models for extreme series including infrequent phenomena, *Hydrological Sciences Journal*, 63:13-14, 1927-1940, DOI: 10.1080/02626667.2018.1546956
- Lenderink, G., and E. van Meijgaard (2008), Increase in hourly precipitation extremes beyond expectations from temperature changes, *Nat. Geosci.*, 1, 511–514.
- Libertino A., Ganora D., & Claps P. (2019). Evidence for increasing rainfall extremes remains elusive at large spatial scales: The case of Italy. *Geophysical Research Letters*, 46, 7437–7446. <https://doi.org/10.1029/2019GL083371>
- Mann, H. B. (1954) Non-parametric tests against trend. *Econometrica* 1945, 13, 245-259.
- Marani M., Ignaccolo M. (2015). A metastatistical approach to rainfall extremes, *Advances in Water Resources*, Volume 79, 2015, Pages 121-126, ISSN 0309-1708, <https://doi.org/10.1016/j.advwatres.2015.03.001>.
- Marchi L., Borga M., Preciso E., Gaume E. (2010). Characterisation of selected extreme flash floods in Europe and implications for flood risk management. *J. Hydrol.*, 394, pp. 118-133, <https://doi.org/10.1016/j.jhydrol.2010.07.017>
- Markonis, Y., Papalexiou, S. M., Martinkova, M., & Hanel, M. (2019). Assessment of water cycle intensification over land using a multi source global gridded precipitation dataset. *Journal of Geophysical Research: Atmospheres*, <https://doi.org/10.1029/2019JD030855>
- Marra, F., Armon, M., Adam, O., Zocatelli, D., Gazal, O., Garfinkel, C. I., et al. (2021). Towards narrowing uncertainty in future projections of local extreme precipitation. *Geophysical Research Letters*, 48, e2020GL091823. <https://doi.org/10.1029/2020GL091823>
- Marra, F., Nikolopoulos, E. I., Anagnostou, E. N., & Morin, E. (2018). Metastatistical extreme value analysis of hourly rainfall from short records: Estimation of high quantiles and impact of measurement errors. *Advances in Water Resources*, 117, 27–39. <https://doi.org/10.1016/j.advwatres.2018.05.001>
- Marra, F., Zocatelli, D., Armon, M., & Morin, E. (2019). A simplified MEV formulation to model extremes emerging from multiple nonstationary underlying processes. *Advances in Water Resources*, 127, 280–290. <https://doi.org/10.1016/j.advwatres.2019.04.002>

- Marra, F., Borga, M., & Morin, E. (2020). A unified framework for extreme subdaily precipitation frequency analyses based on ordinary events. *Geophysical Research Letters*, 47, e2020GL090209.
- Min SK, Zhang X, Zwiers F, Friederichs P, Hense A (2009) Signal detectability in extreme precipitation changes assessed from twentieth century climate simulations. *Clim Dyn* 32:95–111
- Miniussi, A., & Marani, M. (2020). Estimation of daily rainfall extremes through the metastatistical extreme value distribution: Uncertainty minimization and implications for trend detection. *Water Resources Research*, 56, e2019WR026535. <https://doi.org/10.1029/2019WR026535>
- Miniussi, A., Villarini, G., & Marani, M. (2020). Analyses through the metastatistical extreme value distribution identify contributions of tropical cyclones to rainfall extremes in the eastern United States. *Geophysical Research Letters*, 47, e2020GL087238. <https://doi.org/10.1029/2020GL087238>
- Moustakis, Y., Papalexiou, S. M., Onof, C. J., & Paschalis, A. (2021). Seasonality, intensity, and duration of rainfall extremes change in a warmer climate. *Earth's Future*, 9, e2020EF001824. <https://doi.org/10.1029/2020EF001824>
- Myhre, G., Alterskjær, K., Stjern, C.W. et al. Frequency of extreme precipitation increases extensively with event rareness under global warming. *Sci Rep* 9, 16063 (2019). <https://doi.org/10.1038/s41598-019-52277-4>
- Papalexiou, S. M., AghaKouchak, A., & Foufoula-Georgiou, E. (2018). A diagnostic framework for understanding climatology of tails of hourly precipitation extremes in the United States. *Water Resources Research*, 54(9), 6725–6738. <https://doi.org/10.1029/2018WR022732>
- Papalexiou, S. M., & Montanari, A. (2019). Global and regional increase of precipitation extremes under global warming. *Water Resources Research*, 55, 4901–4914. <https://doi.org/10.1029/2018WR024067>
- Paprotny, D., Sebastian, A., Morales-Napoles, O., & Jonkman, S. N. (2018). Trends in flood losses in Europe over the past 150 years. *Nature Communications*, 9, 1985
- Pendergrass, A. G. (2018). What precipitation is extreme? *Science*, 360, 6393. <https://doi.org/10.1126/science.aat1871>
- Pendergrass, A.G. (2020). Changing Degree of Convective Organization as a Mechanism for Dynamic Changes in Extreme Precipitation. *Curr Clim Change Rep* 6, 47–54. <https://doi.org/10.1007/s40641-020-00157-9>
- Pendergrass, A. G., Hartman, D. L. (2014). The Atmospheric Energy Constraint on Global-Mean Precipitation Change. *J. Climate*, 27, 2, 757-768, <https://doi.org/10.1175/JCLI-D-13-00163.1>
- Prosdociimi, I., Kjeldsen, T. Parametrisation of change-permitting extreme value models and its impact on the description of change. *Stoch Environ Res Risk Assess* 35, 307–324 (2021). <https://doi.org/10.1007/s00477-020-01940-8>

- 488 Rossi, F., Fiorentino, M., and Versace, P. (1984), Two-Component Extreme Value Distribution  
489 for Flood Frequency Analysis, *Water Resour. Res.*, 20( 7), 847– 856,  
490 doi:10.1029/WR020i007p00847.
- 491 Schär C., N. Ban, E.M. Fischer, et al., 2016. Percentile indices for assessing changes in heavy  
492 precipitation events. *Clim. Change*, 137, 201-216, [https://doi.org/10.1007/s10584-016-](https://doi.org/10.1007/s10584-016-1669-2)  
493 1669-2
- 494 Sen PK (1968). Estimates of the regression coefficient based on Kendall's tau, *J. Am. Statist.*  
495 *Assoc.*, 63, 1379–1389, <http://doi.org/10.1080/01621459.1968.10480934>
- 496 Serinaldi, F., & Kilsby, C. G. (2015). Stationarity is undead: Uncertainty dominates the  
497 distribution of extremes. *Advances in Water Resources*, 77, 17–36.
- 498 Trenberth, K. E., A. Dai, R. M. Rasmussen, and D. B. Parsons (2003), The changing character of  
499 precipitation, *Bull. Am. Meteorol. Soc.*, 84, 1205– 1217.
- 500 van Belle G., Hughes, J. P. (1984) Nonparametric tests for trend in water quality. *Water Resour.*  
501 *Res.* 1984, 20, 127-136.
- 502 Zheng F., Westra S., Leonard M. (2015). Opposing local precipitation extremes. *Nature Clim*  
503 *Change* 5, 389–390. <https://doi.org/10.1038/nclimate2579>
- 504 Zorzetto E., Botter G., Marani M. (2016). On the emergence of rainfall extremes from ordinary  
505 events. *Geophysical Research Letters*, 43, 8076–8082.  
506 <https://doi.org/10.1002/2016GL069445>



*Geophysical Research Letters*

Supporting Information for

**Enhanced summer convection explains observed trends in extreme subdaily precipitation in the northeastern Italian Alps**

E. Dallan<sup>1</sup>, M. Borga<sup>1</sup>, M. Zaramella<sup>1</sup>, F. Marra<sup>2</sup>

<sup>1</sup> Department of Land Environment Agriculture and Forestry, University of Padova, Padova, Italy

<sup>2</sup> National Research Council of Italy - Institute of Atmospheric Sciences and Climate (CNR-ISAC), Bologna, Italy

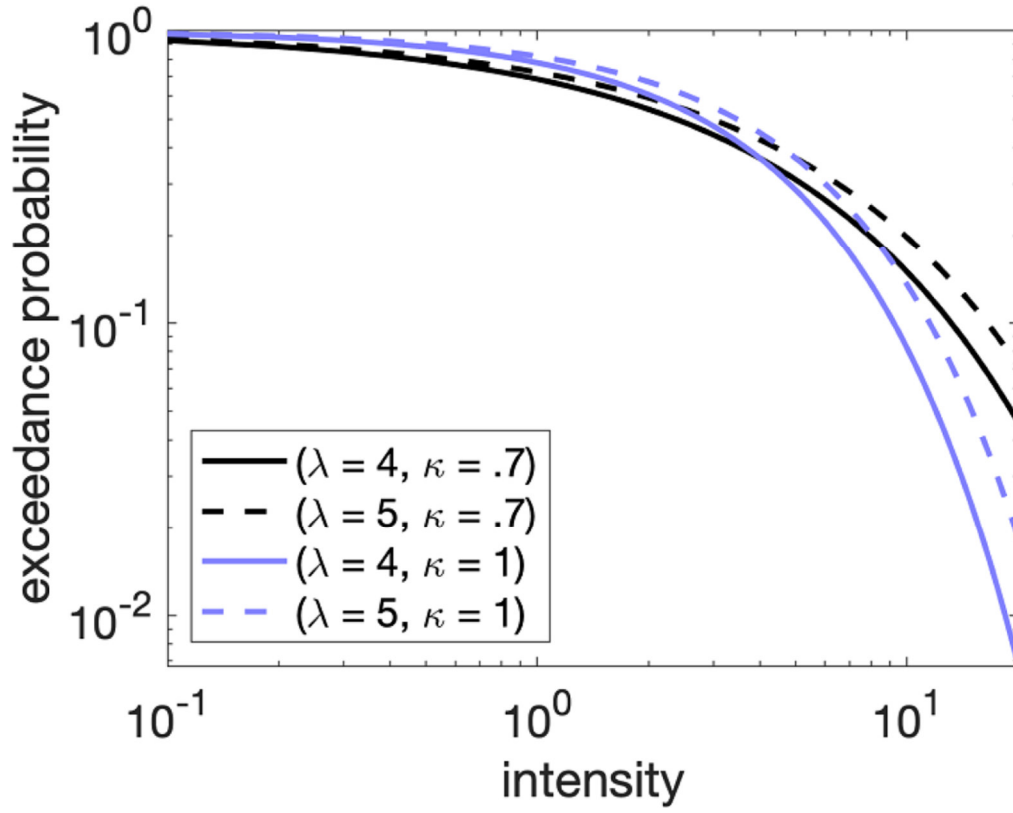
**Contents of this file**

Table S1

Figures S1 to S2

Code	Name	X [m]	Y [m]	Quote [m a.s.l.]	# years
T0010	Levico (Terme)	678457	5097800	502	28
T0014	Telve (Pontarso)	692750	5109940	925	28
T0015	Bieno	697716	5106240	843	29
T0024	Passo Cereda	724970	5119950	1322	30
T0030	Canal San Bovo	711191	5114300	750	28
T0032	Lavarone (Chiesa)	674697	5089880	1155	29
T0071	Mezzana	638273	5130430	905	30
T0074	Male'	647602	5134900	720	27
T0082	Passo Mendola	668239	5142950	1315	29
T0092	Pian Fedaia (Diga)	719834	5149030	2063	29
T0096	Moena (Diga Pezze')	704896	5140120	1205	30
T0103	Passo Rolle	714648	5130920	2012	29
T0104	Passo Valles	715465	5135460	2032	29
T0115	Segonzano (Gresta)	676612	5120060	660	28
T0118	Cembra	671193	5115370	652	27
T0139	Sant'Orsola Terme	677921	5108520	925	30
T0146	Aldeno (San Zeno)	662021	5092620	182	29
T0147	Rovereto	658565	5084560	203	29
T0148	Terragnolo (Piazza)	666927	5082920	800	28
T0151	Mori (Loppio)	649939	5079790	230	28
T0153	Ala (Ronchi)	660682	5067140	692	28
T0177	Val di Breguzzo (Ponte Arno')	626962	5098910	1148	27
T0179	Tione	633926	5100070	533	30
T0182	Montagne (Larzana)	635493	5102100	955	28
T0189	Santa Massenza (Centrale)	653156	5103200	252	29
T0193	Torbole (Belvedere)	645707	5081330	90	29
T0203	Forte D'Ampola	627788	5080240	740	27
T0210	Folgaria	667845	5086920	1121	28
T0212	Spormaggiore	657859	5120520	555	28
T0236	Romeno	662908	5139640	958	30

**Table S1.** Rain gauge stations. Coordinates X and Y are in WGS 84/UTM zone 32N Reference System.



**Figure S1.** Exceedance probability of Weibull distributions with different scale ( $\lambda$ ) and shape ( $\kappa$ ) parameters. Blue lines show the case with exponential tail  $\kappa = 1$ ; black lines show a case with heavier tail ( $\kappa = 0.7$ ). Dashed lines show higher scale parameters ( $\lambda = 5$ ) while solid lines show lower scale parameters ( $\lambda = 4$ ).

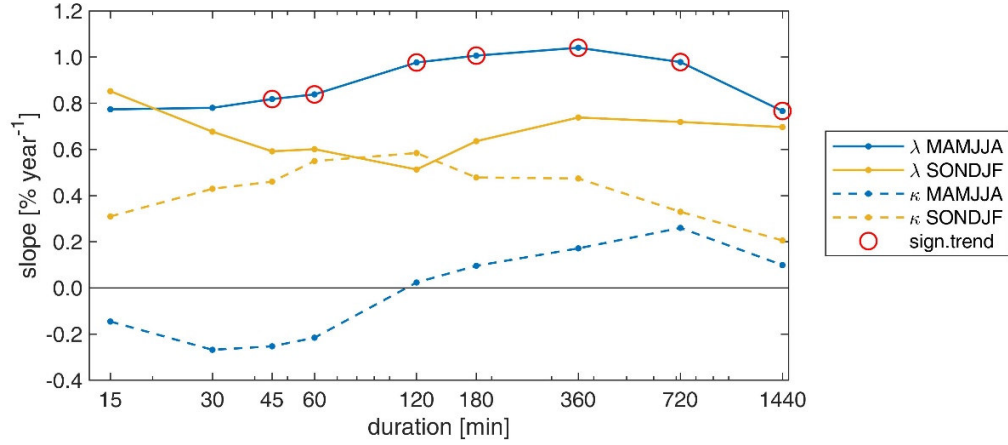


**Figure S2.** Scale  $\lambda$  and shape  $\kappa$  trend slopes for two seasons. The trend analysis on the distribution parameters is here performed to evaluate their changes for the different seasons. Because of the low sample size, this analysis is performed by dividing the annual events in two “seasons”, aggregating MAM with JJA and SON with DJF. For all the seasons and durations, the scale parameter increases, with significant trends in MMA-JJA. This resembles the behavior of the whole-year parameters reported in Figure 2 in the main manuscript. Interestingly, the shape parameter shows positive trends (decreasing tail heaviness) in SON-DJF, and opposing trends at short and long durations in MMA-JJA. Decreasing trends are observed for durations  $\leq 2$  h and increasing trends for durations  $\geq 3$  h (increasing and decreasing tail heaviness, respectively). The overall decreasing trend at short durations, that was observed for the whole-year and that dominates the overall response of annual maxima, is thus imputable to the period MMA-JJA.